Electronic Supplementary Information

Controlling the efficient and ultralong room-temperature phosphorescence of 9*H*-dibenzo[*a*,*c*]carbazole derivatives for erasable light printing

Wei Cai‡, Lingqi Zuo‡, Shiya Feng, Pengtao Hu, Hengshan Wei, Zhexian Zhang, Hongru Wu, Leyu Wang*, Yuhai Wang, Guang Shi*, Bingjia Xu*

[a] *Guangdong Tloong Ink Co., Ltd., Zhaoqing 526000, China. E-mail: wly@tlym.cn*

[b] *School of Chemistry, South China Normal University, Guangzhou 510006, China. E-mail: bingjiaxu@m.scnu.edu.cn, shg73@163.com*

‡ These authors contributed equally to this work.

Contents

I. Experimental section

Chemical Reagents and Materials

Benzene sulfonyl chloride (99%), bromobenzene (99.5%), tris(dibenzylideneacetone) dipalladium(0) (98%), 1,3-propylenediamine (98%), potassium *tert*-butoxide (98%), and 2-dicyclohexylphosphino-2′,6′-diisopropoxybiphenyl (98%) were purchased from *Energy Chemistry*. Bisphenol A diglycidyl ether (BADGE) was purchased from NIPPON STEEL (Japan, HPLC 100%). 2-Bromodibenzo[*b*,*d*]thiophene (98%) and 9*H*-dibenzo[*a*,*c*]carbazole (97%) were purchased from *Bidepharm*. Other reagents and organic solvents were purchased from Guangzhou *Zeyuan* Company (China) with analytical grade and used without further purification.

Instruments and Measurements

^{1}H and ^{13}C nuclear magnetic resonance spectra (^{1}H NMR and ^{13}C NMR) of the intermediates and the final products were obtained on a Bruker AVANCE spectrometer (600 MHz) by employing $CDCl_3$ and DMSO-d_6 as solvents and tetramethylsilane as internal standard. High-resolution mass spectrometry was carried out on the instrument of LTQ_Orbitrap_LCMS (LTQ Orbitrap Elite) to determine the exact molecular weights of the compounds. FT-IR spectra were recorded on the instrument Perkin-Elmer Spectrum II. Thermogravimetric analyses (TGA) were carried out using a thermal analyzer (Shimadzu, TGA-50H) under N_2 gas flow with a heating rate of 10 °C/min. Differential scanning calorimetry (DSC) curves were achieved using a TA Q20 thermal analyzer at a heating rate of 10 ºC/min under a nitrogen atmosphere. In addition, steady-state PL spectra, delayed emission spectra, absolute PL quantum yields, and time-resolved emission decay curves were collected using a spectrometer (FLS980) equipped with a calibrated integrating sphere and a thermostat (Oxford) from Edinburgh Instruments. The afterglow images of the samples were all picked out from Videos. The calculation method for the phosphorescence quantum yields of the polymer films is similar to the ones reported in previous references.[1-3] Taking BCzS-EP-0.05% as an example, its phosphorescence spectrum is first normalized to match the steady-state one in the long wavelength region. Afterward, its phosphorescence quantum yield can be calculated by using the following

equation:

$$\Phi_{phos.} = \frac{B}{A} \times \Phi_{PL}$$

Where A, B, Φ_{PL}, and $\Phi_{phos.}$ represent the area of the steady-sate PL spectrum, the area of the phosphorescence spectrum, the total PL quantum yield, and the phosphorescence quantum yield, respectively.

Theoretical calculations

The molecular geometries of 9-(dibenzo[*b*,*d*]thiophen-2-yl)-9*H*-dibenzo[*a*,*c*]carbazole (BCzS) and 9-(4-(phenylsulfonyl)phenyl)-9*H*-dibenzo[*a*,*c*]carbazole (BCzSF) at ground state were optimized using the density functional theory (DFT) method at the B3LYP/6-311G* level in the Gaussian 09 program.[4] On the basis of this, exciton energies in singlet (S_n) and triplet states (T_n) were estimated through a combination of time-dependent DFT (TD-DFT) and B3LYP at the 6-311G* level in the Gaussian 16 program. Spin-orbit coupling (SOC) matrix elements between the singlet and triplet excited states were calculated through the ORCA software based on the TD-DFT results.[5] Natural transition orbital (NTO) analysis was performed based on the TD-DFT results and subsequently extracted by Multiwfn (version 3.8) and then visualized via VMD (version 1.9.3).[6, 7]

Synthesis

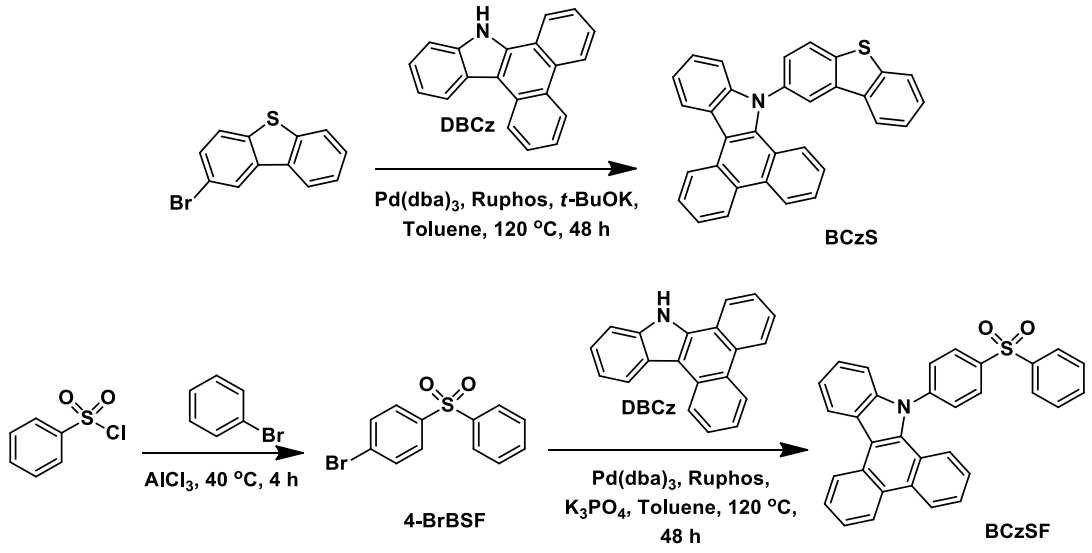

Scheme S1. The synthetic routes of BCzS and BCzSF.

1-Bromo-4-(phenylsulfonyl)benzene (4-BrBSF) was synthesized according to the method

reported in literature.[8]

Synthesis of 9-(dibenzo[*b*,*d*]thiophen-2-yl)-9*H*-dibenzo[*a*,*c*]carbazole (BCzS) To a solution of 9*H*-dibenzo[*a*,*c*]carbazole (0.20 g, 0.75 mmol) in toluene (25 mL), 2-bromodibenzo[*b*,*d*]thiophene (0.39 g, 1.50 mmol), potassium *tert*-butoxide (0.42 g, 3.75 mmol), and 2-dicyclohexylphosphino-2′,6′-diisopropoxybiphenyl (Ruphos, 0.16 g, 0.34 mmol) were added. After bubbling with argon for 30 min, tris(dibenzylideneacetone) dipalladium(0) (0.05 g, 0.09 mmol) was added. Subsequently, the resulting mixture was stirred at 120 ºC for 48 h under an argon atmosphere. After cooling to room temperature, the mixture was filtered, and the filtrate solvent was removed by rotary evaporation. The crude product was then separated and purified by silica gel column chromatography using dichloromethane and petroleum ether (*v*/*v*=1:2) as eluent. The resulting powder was further reprecipitated from dichloromethane/methanol under the action of ultrasonic to give a white solid powder (0.04 g, yield 11.9 %). ^{1}H NMR (600 MHz, $CDCl_3$) δ 9.03-8.98 (d, 1H), 8.87-8.81 (d, 2H), 8.75-8.70 (d, 1H), 8.38-8.36 (s, 1H), 8.18-8.14 (d, 1H), 8.14-8.09 (d, 1H), 8.02-7.94 (d, 1H), 7.88-7.81 (t, 1H), 7.65-7.69 (t, 1H), 7.64-7.60 (d, 1H), 7.59-7.55 (m, 3H), 7.51-7.45 (m, 2H), 7.43-7.39 (t, 1H), 7.27-7.22 (m, 2H). ^{13}C NMR (151 MHz, $CDCl_3$) δ 142.50, 140.38, 139.84, 137.27, 137.04, 135.03, 134.75, 130.90, 129.91, 128.59, 127.56, 127.44, 127.40, 126.09, 125.78, 124.82, 124.47, 124.11, 124.04, 123.87, 123.59, 123.26, 123.20, 123.04, 122.12, 122.04, 121.76, 121.19, 114.34, 111.04. ESI-MS m/z: $[M+H]^+$ calcd. for $C_{32}H_{20}NS^+$,450.13110; found, 450.13141.

Synthesis of 9-(4-(phenylsulfonyl)phenyl)-9*H*-dibenzo[*a*,*c*]carbazole (BCzSF) To a solution of 9*H*-dibenzo[*a*,*c*]carbazole (0.20 g, 0.75 mmol) in toluene (25 mL), 4-BrBSF (0.45 g, 1.51 mmol), potassium phosphate (0.80 g, 3.75 mmol), and 2-dicyclohexylphosphino-2′,6′-diisopropoxybiphenyl (0.16 g, 0.34 mmol) were added. After bubbling with argon for 30 min, tris(dibenzylideneacetone) dipalladium(0) (0.05 g, 0.09 mmol) was added. Subsequently, the resulting mixture was stirred at 120 ºC for 48 h under an argon atmosphere. After cooling to room temperature, the mixture was filtered, and the filtrate solvent was removed by rotary evaporation. The crude product was then separated and purified by silica gel column chromatography using dichloromethane and petroleum

ether (*v*/*v*=1:2) as eluent. The resulting powder was further reprecipitated from dichloromethane/methanol under the action of ultrasonic to give a white solid powder (0.21 g, yield 58.3 %). ^{1}H NMR (600 MHz, DMSO-d_6) δ 9.08-8.96 (m, 3H), 8.77-8.73 (d, 1H), 8.33-8.28 (d, 2H), 8.14-8.10 (m, 2H), 7.90-7.88 (d, 2H), 7.88-7.84 (t, 1H), 7.82-7.78 (t, 1H), 7.76-7.72 (t, 2H), 7.72-7.68 (t, 1H), 7.66-7.62 (t, 1H), 7.48-7.44 (t, 1H), 7.44-7.40 (t, 1H), 7.35-7.32 (t, 1H), 7.26-7.22 (d, 1H), 7.22-7.18 (t, 1H). ^{13}C NMR (151 MHz, $CDCl_3$) δ 144.98, 141.64, 141.59, 141.14, 134.20, 133.65, 130.92, 129.65, 129.56, 129.48, 127.92, 127.67, 127.55, 126.15, 126.01, 124.49, 124.42, 124.08, 123.87, 123.60, 123.13, 122.61, 121.99, 121.80, 115.50, 110.54. ESI-MS m/z: $[M+H]^+$ calcd. for $C_{32}H_{22}NO_2S^+$,484.13658; found, 484.13687.

General procedures for the preparation of the blank and doped epoxy polymer films

BCzS (3.96 mg, 8.80×10^{-3} mmol) was added to a mixture of bisphenol A diglycidyl ether (300.00 mg, 0.88 mmol) and 1,3-propanediamine (65.20 mg, 0.88 mmol, 72.0 μL). The resulting mixture was stirred at room temperature for about 1 min and then coated on a glass slide. After curing at 90 ºC for 5 h, the EP film with a dopant concentration of 1.00% (BCzS-EP-1.00%) was obtained. Similarly, the bland EP, BCzS-EP-0.50%, and BCzS-EP-0.10% films could be prepared by adding 0, 1.98, and 0.39 mg of BCzS to the mixtures, respectively.

On the other hand, BCzS (1.00 mg, 1.73×10^{-3} mmol) was dissolved in dichloromethane (1.0 mL) to prepare a stock solution. Subsequently, 198 and 39 μL of the stock solution were added to the mixtures of bisphenol A diglycidyl ether (300.00 mg, 0.88 mmol) and 1,3-propanediamine (65.20 mg, 0.88 mmol, 72.0 μL), respectively. The resulting mixtures were stirred at room temperature for about 1 min and then coated on a glass slide. Finally, they were cured at 90 ºC for 5 h to give the EP films with dopant concentrations of 0.05% and 0.01% (BCzS-EP-0.05% and BCzS-EP-0.01%).

The EP films with different dopant concentrations of BCzSF were prepared by the same methods.

II. Photophysical Properties of the Guest Compounds and Their Epoxy Polymer Films

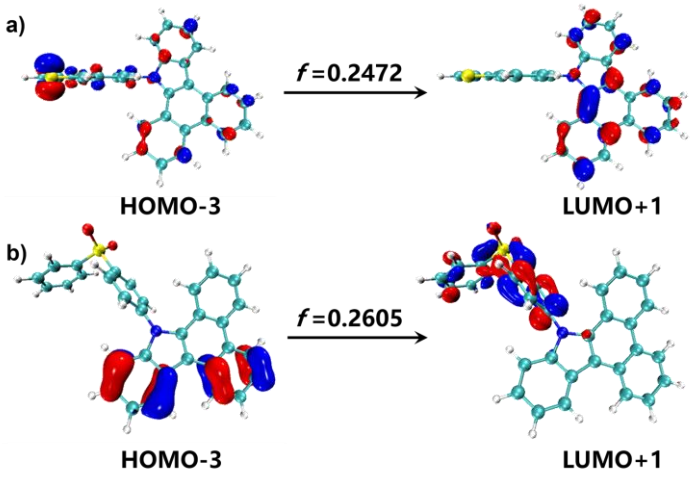

Figure S1. Kohn–Sham frontier orbitals of the BCzS (a) and BCzSF (b) molecules after optimization. *f* represents the oscillator strength, and the percentage is the corresponding transition probability.

Table S1. Energy levels and spin-orbit coupling constants of the singlet and triplet excited states of BCzS and BCzSF

BCzS				BCzSF			
Excited State	**Energy Level (eV)**	**SOC Constant (cm^{-1})**		**Excited State**	**Energy Level (eV)**	**SOC Constant (cm^{-1})**	
S_1	3.285			S_1	3.159		
T_1	2.632	S_0	0.09	T_1	2.600	S_0	0.22
		S_1	0.37			S_1	0.44
T_2	3.149	S_1	0.26	T_2	3.098	S_1	0.14
T_3	3.158	S_1	0.12	T_3	3.202	S_1	0.08
T_4	3.224	S_1	0.07	T_4	3.331	S_1	0.14
T_5	3.356	S_1	0.22	T_5	3.413	S_1	0.33
T_6	3.482	S_1	0.21	T_6	3.553	S_1	
T_7	3.520	S_1	0.16	T_7	3.663	S_1	
T_8	3.652	S_1		T_8	3.692	S_1	
T_9	3.741	S_1		T_9	3.718	S_1	
T_{10}	3.770	S_1		T_{10}	3.764	S_1	

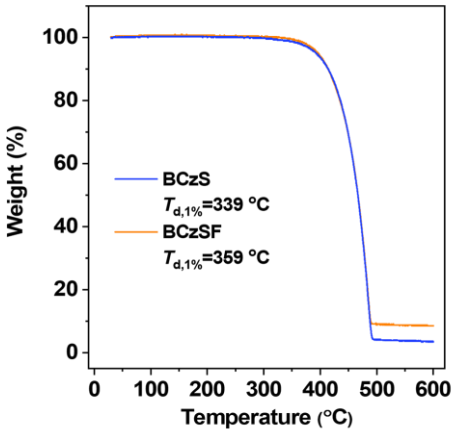

Figure S2. Thermogravimetic analysis curves of BCzS and BCzSF under nitrogen.

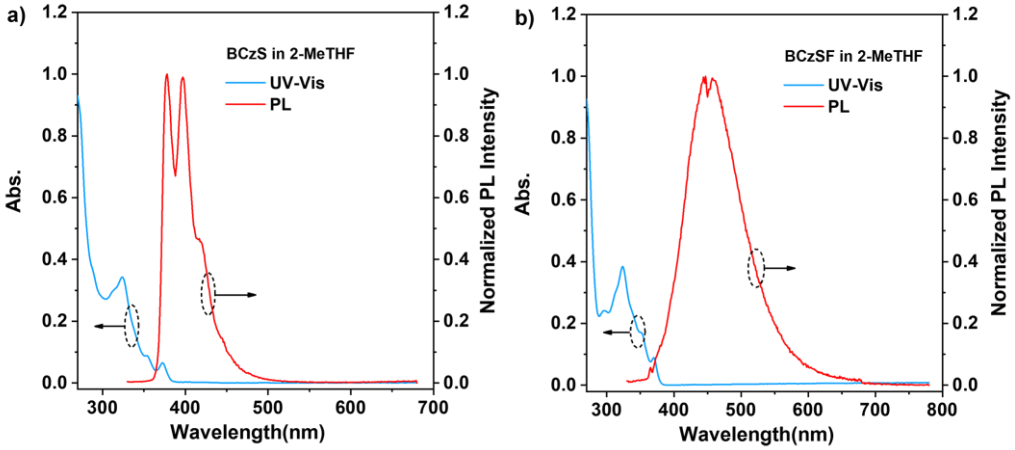

Figure S3. UV-visible absorption and PL spectra of the BCzS a) and BCzSF b) in 2-MeTHF at room temperature. (Concentration: 10 μM)

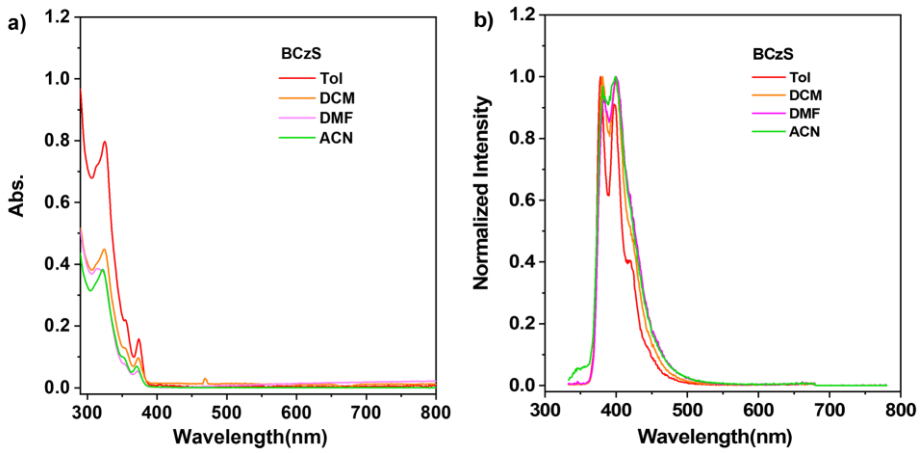

Figure S4. UV-visible absorption a) and PL b) spectra of the BCzS in different solvents at room temperature (Concentration: 10 μM). Tol, DCM, DMF, and ACN represent toluene, dichloromethane, *N*,*N*′-dimethylformamide, and acrylonitrile, respectively.

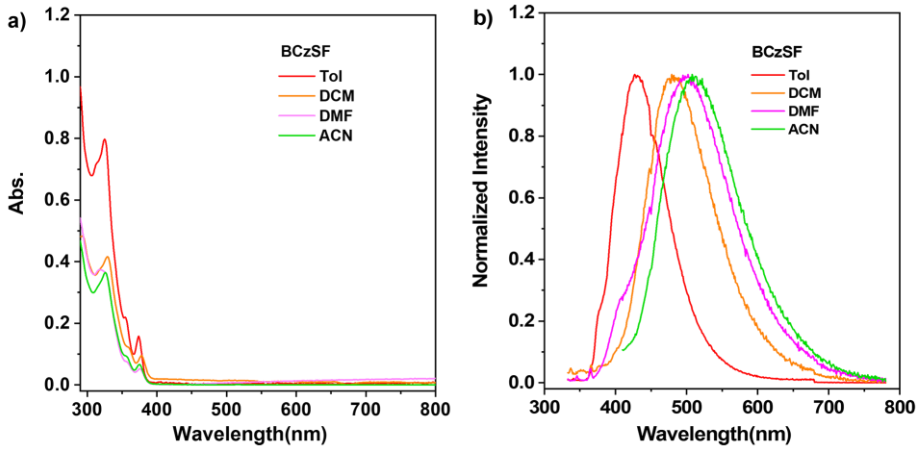

Figure S5. UV-visible absorption a) and PL b) spectra of the BCzSF in different solvents at room temperature (Concentration: 10 μM). Tol, DCM, DMF, and ACN represent toluene, dichloromethane, *N*,*N*′-dimethylformamide, and acrylonitrile, respectively.

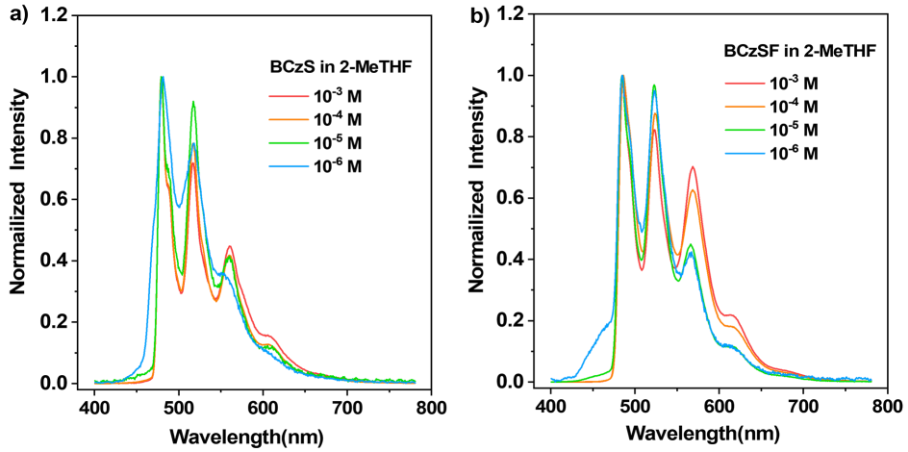

Figure S6. Phosphorescence emission spectra of the BCzS a) and BCzSF b) in 2-MeTHF with different concentrations at 77 K.

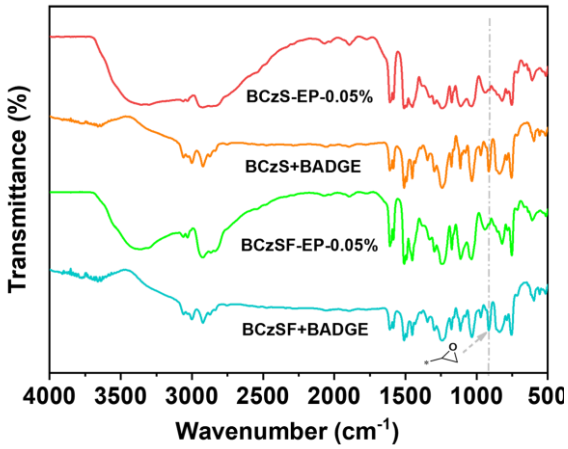

Figure S7. FT-IR spectra of the polymer films and the mixtures of BADGE with BCzS and BCzSF.

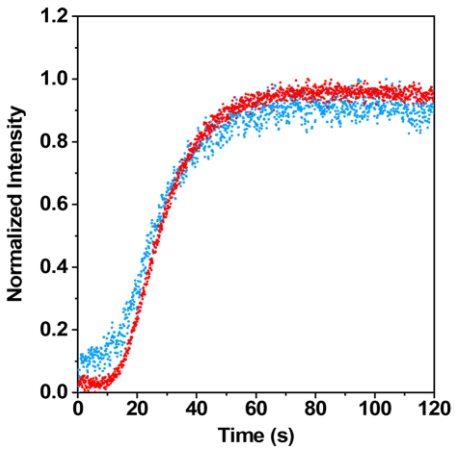

Figure S8. Normalized phosphorescence intensities of the BCzS-EP-0.05% and BCzSF-EP-0.05% films against time upon continuous UV irradiation (0.4 mW/cm^2).

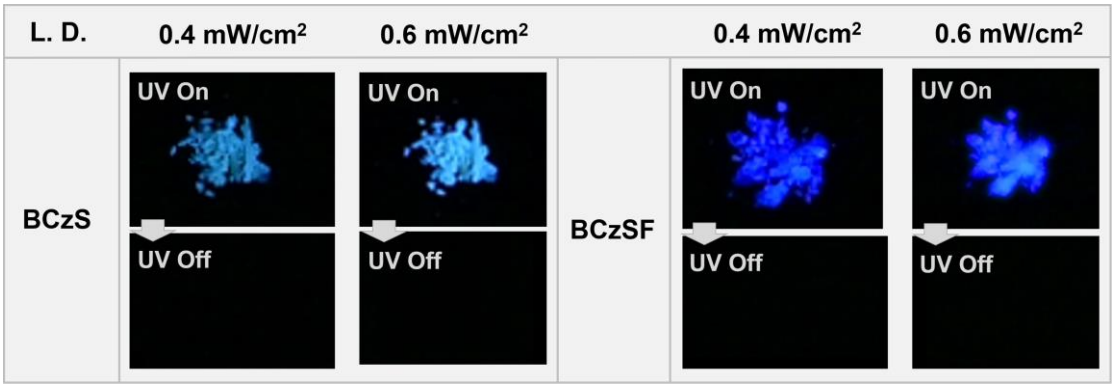

Figure S9. Luminescence properties of the crystalline samples of BCzS and BCzSF after the irradiation of 365 nm UV light with different light densities. L. D. means light density. (0.4 mW/cm^2 for 1 min and 0.6 mW/cm^2 for 3 min)

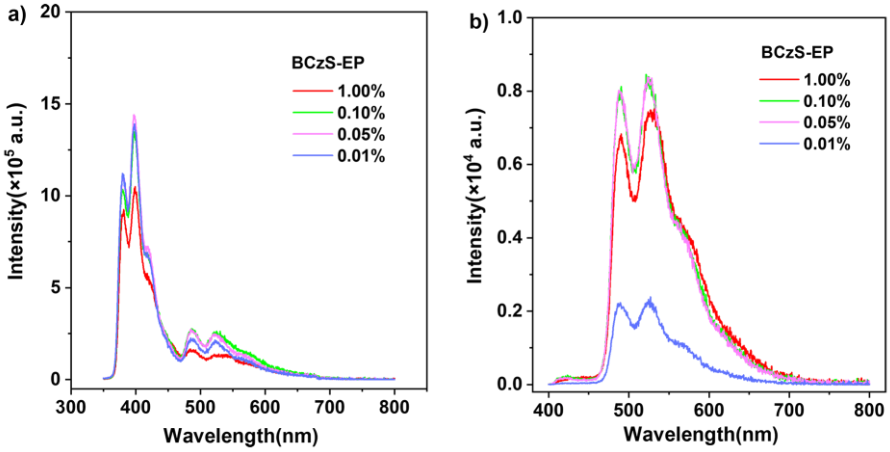

Figure S10. Steady-state a) and delayed b) PL spectra of the BCzS-EP films under ambient conditions.

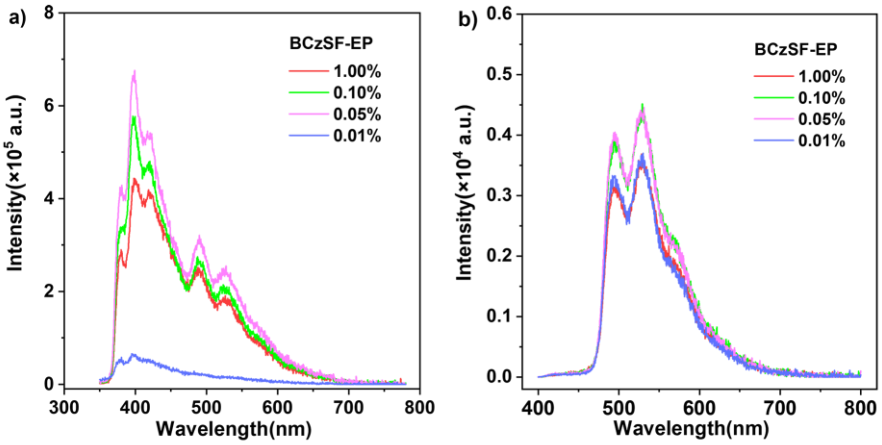

Figure S11. Steady-state a) and delayed b) PL spectra of the BCzSF-EP films under ambient conditions.

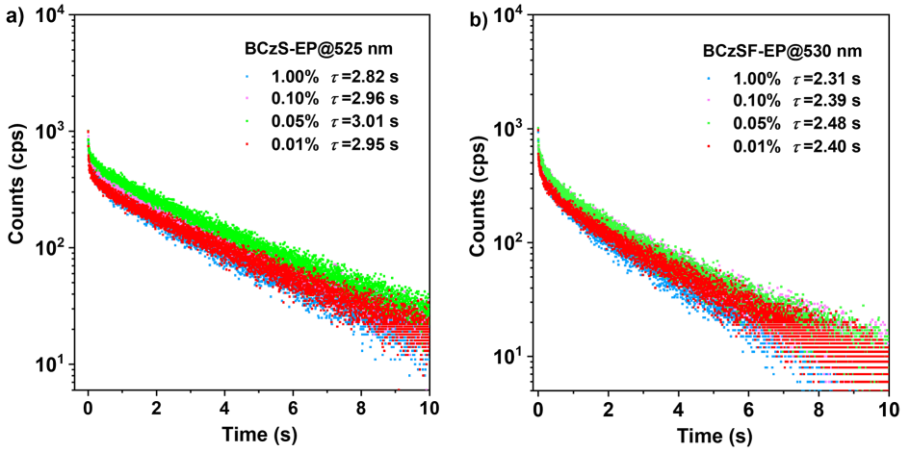

Figure S12. Emission decay curves of the BCzS-EP a) and BCzSF-EP b) films with different dopant concentrations under ambient conditions.

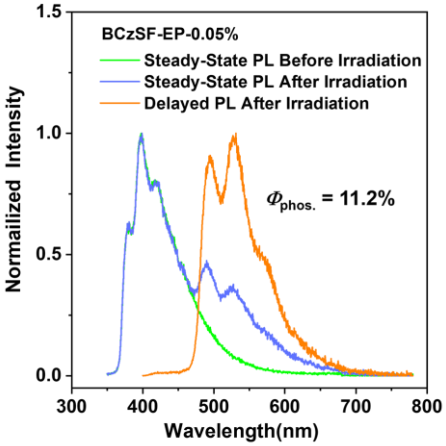

Figure S13. Steady-state and delayed PL spectra of the BCzSF-EP-0.05% film before and after light irradiation under ambient conditions.

Table S2. Photophysical properties of the BCzS-EP-0.05% and BCzSF-EP-0.05% films

Sample	λ_{PF} (nm)	τ_{PF} (ns)	$\lambda_{phos.}$ (nm)	$\tau_{phos.}$ (ms) [a]	$\tau_{phos.}$ (s) [b]	Φ_{PL} (%) [b]	$\Phi_{phos.}$ (%) [b]
BCzS-EP-0.05%	398	7.18	525	0.55	3.01	39.0	13.5
BCzS-EP-0.05%	398	6.78	530	1.39	2.40	32.8	11.2

[a] Before photoactivation under ambient conditions; [b] after photoactivation under ambient conditions.

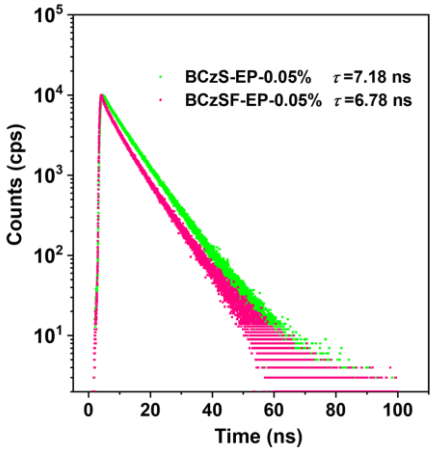

Figure S14. Prompt fluorescence decay curves of the BCzS-EP-0.05% and BCzSF-EP-0.05% films under ambient conditions.

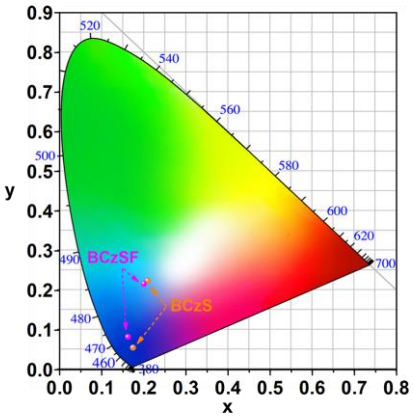

Figure S15. The $CIE_{x,y}$ chromaticity coordinates of BCzS-EP-0.05% and BCzSF-EP-0.05% before and after photoactivation.

As shown in Figure S15, the $CIE_{x,y}$ chromaticity coordinates of BCzS-EP-0.05% before and after photoactivation were determined to be (0.174, 0.056) and (0.209, 0.224), respectively, while the ones of BCzSF-EP-0.05% were (0.162, 0.083) and (0.200, 0.217).

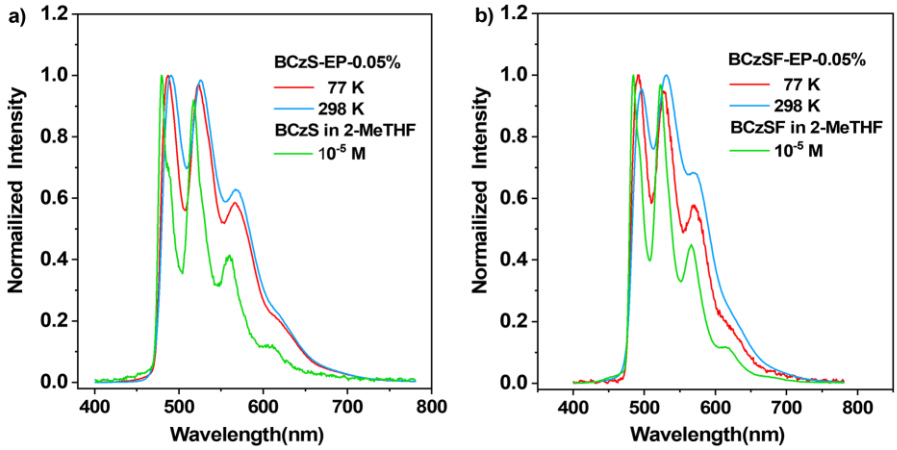

Figure S16. a) Delayed emission spectra of the BCzS-EP-0.05% film at 77 and 298 K, and the phosphorescence emission spectrum of BCzS in 2-MeTHF at 77 K (10 μM). b) Delayed emission spectra of the BCzSF-EP-0.05% film at 77 and 298 K, and the phosphorescence emission spectrum of BCzSF in 2-MeTHF at 77 K (10 μM).

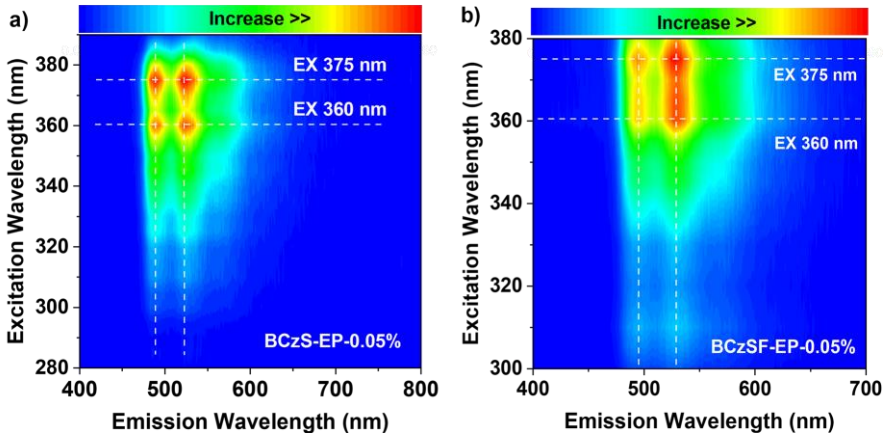

Figure S17. Variations of the delayed emissions of the BCzS-EP-0.05% (a) and BCzSF-EP-0.05% (a) films with the change of excitation wavelength under ambient conditions.

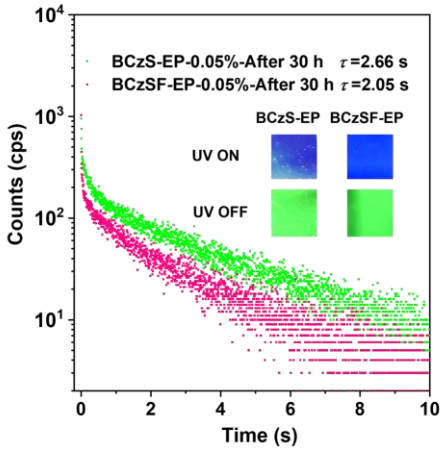

Figure S18. Emission decay curves of the UOP of BCzS-EP-0.05% and BCzSF-EP-0.05% after storing in the air at room temperature for 30 h. The insets are the luminescence images of the polymer films before and after removing the excitation light source.

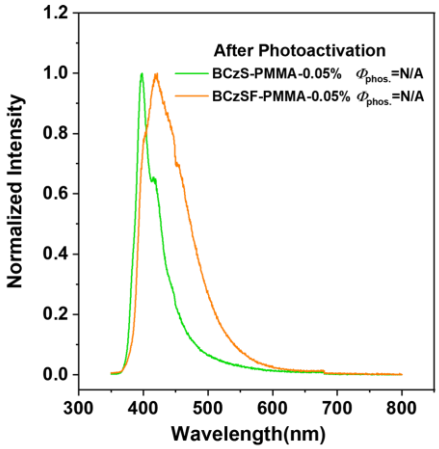

Figure S19. Steady-state PL spectra of the BCzS-PMMA-0.05% and BCzSF-PMMA-0.05% under ambient conditions.

It is found that BCzS and BCzSF showed an emission maximum at around 397 and 419 nm in the PMMA matrices, respectively. However, their phosphorescence quantum yields under ambient conditions are not available because the UOP bands are completely covered by the fluorescence ones. As compared to the doped EP films, BCzS-PMMA-0.05% and BCzSF-PMMA-0.05% exhibited much weaker organic afterglow at room temperature after photoactivation, suggesting their relatively poor UOP performance.

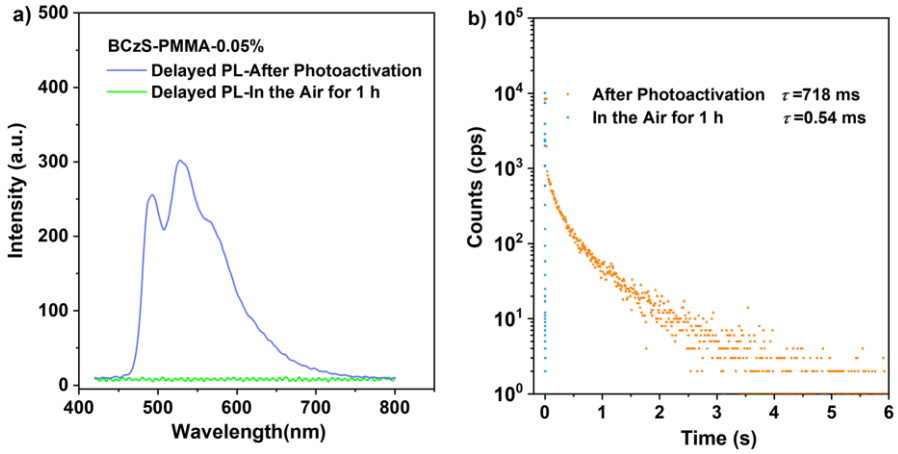

Figure S20. Delayed Emission spectra (8 ms delay) a) and decayed curves of the delayed emissions b) of the BCzS-PMMA-0.05% film after photoactivation and then stored in the air at room temperature for 1 h.

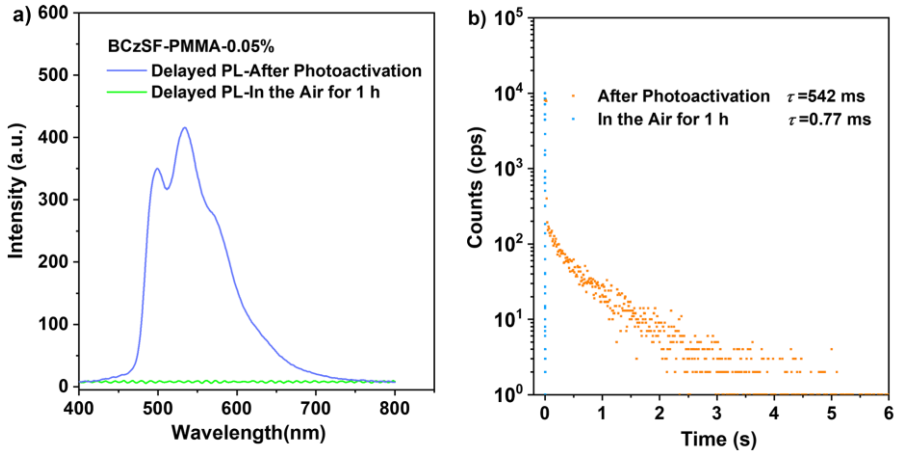

Figure S21. Delayed Emission spectra (8 ms delay) a) and decayed curves of the delayed emissions b) of the BCzSF-PMMA-0.05% film after photoactivation and then stored in the air at room temperature for 1 h.

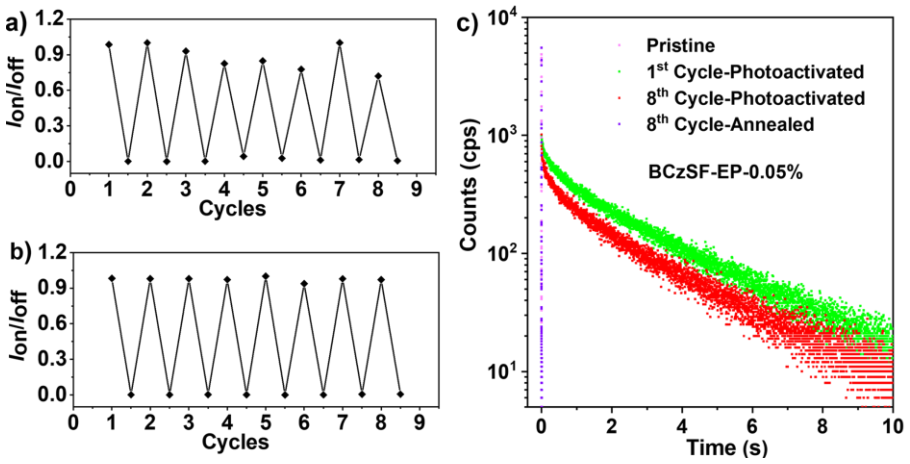

Figure S22. a) Switching of the phosphorescence intensity of BCzS-EP-0.05% upon photoactivation and thermal annealing. I_{on} represents the phosphorescence intensity at 525 nm after photoactivation, while I_{off} is the one after thermal annealing. b) Switching of the phosphorescence intensity of BCzSF-EP-0.05% upon photoactivation and thermal annealing. I_{on} represents the phosphorescence intensity at 530 nm after photoactivation, while I_{off} is the one after thermal annealing. c) Switching of the phosphorescence lifetimes of BCzSF-EP-0.05% upon photoactivation and thermal annealing at the first and eight cycles.

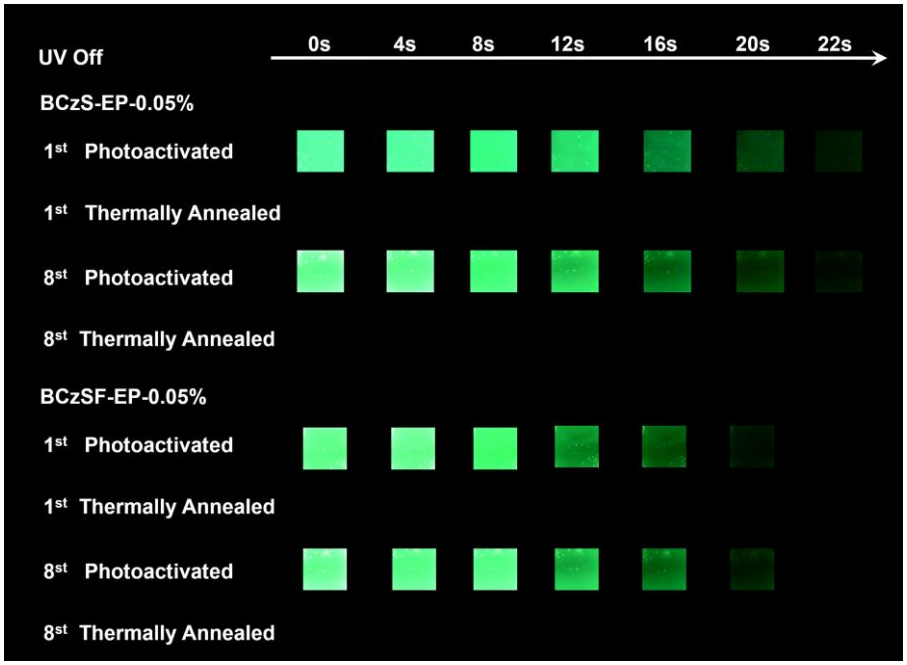

Figure S23. The delayed luminescence images of the BCzS-EP-0.05% and BCzSF-EP-0.05% films after photoactivation and thermal annealing at the first and eight cycles.

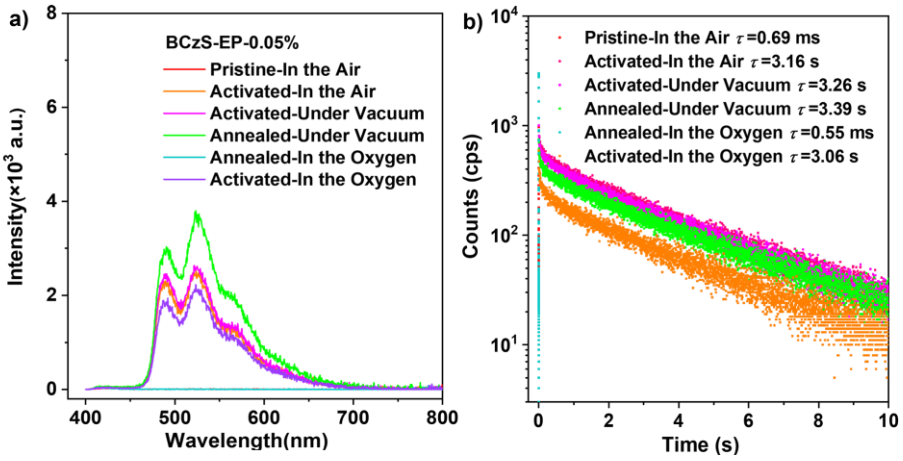

Figure S24. a) Variation of the delayed emission spectra of BCzS-EP-0.05% (1 ms delayed). c) Variation of the emission decay curves of BCzS-EP-0.05%. The photoactivated samples were achieved via illuminating the polymer films at room temperature for 1 min by using 365 nm UV light, while the annealed samples were obtained by heating the polymer film at 120 °C for 10 min and then cool down to 300 K.

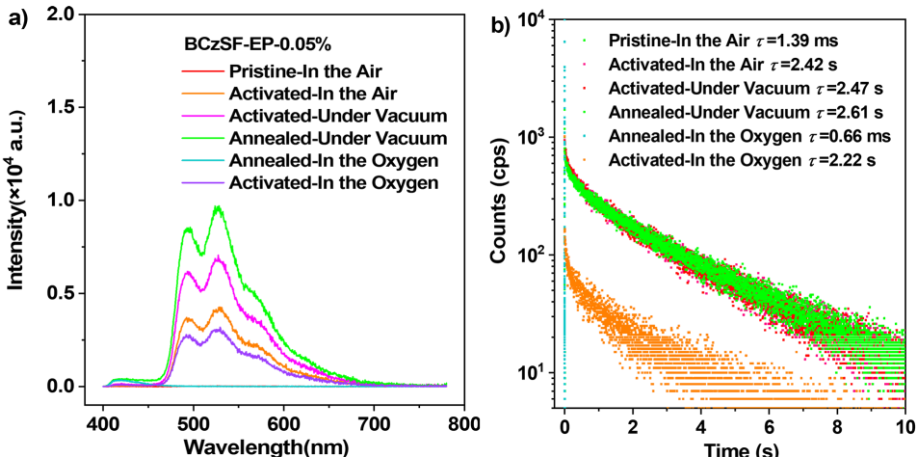

Figure S25. a) Variation of the delayed emission spectra of BCzSF-EP-0.05% (1 ms delayed). c) Variation of the emission decay curves of BCzSF-EP-0.05%. The photoactivated samples were achieved via illuminating the polymer films at room temperature for 1 min by using 365 nm UV light, while the annealed samples were obtained by heating the polymer film at 120 °C for 5 min and then cool down to 300 K.

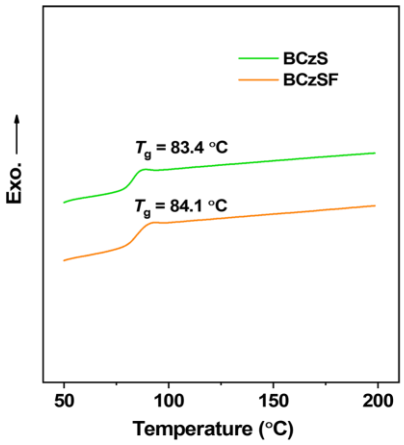

Figure S26. DSC curves of the BCzS-EP-0.05% and BCzSF-EP-0.05% films.

III. ^{1}H NMR, ^{13}C NMR, and Mass Spectra of BCzS and BCzSF

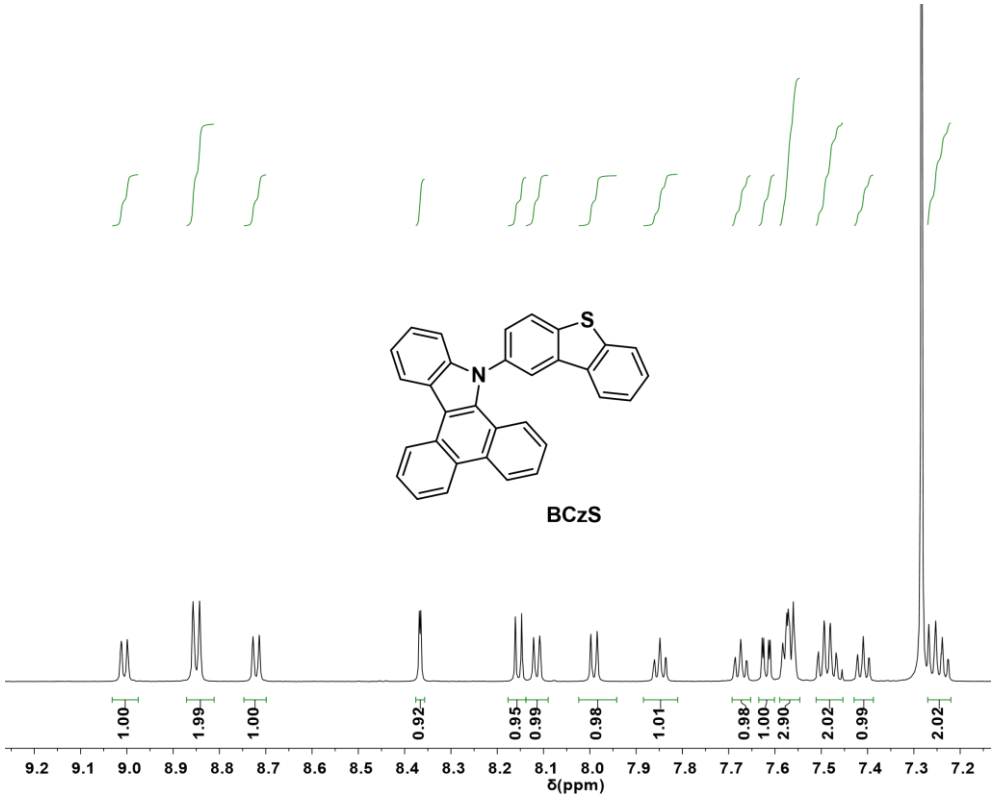

Figure S27. ^{1}H NMR spectrum of the BCzS ($CDCl_3$).

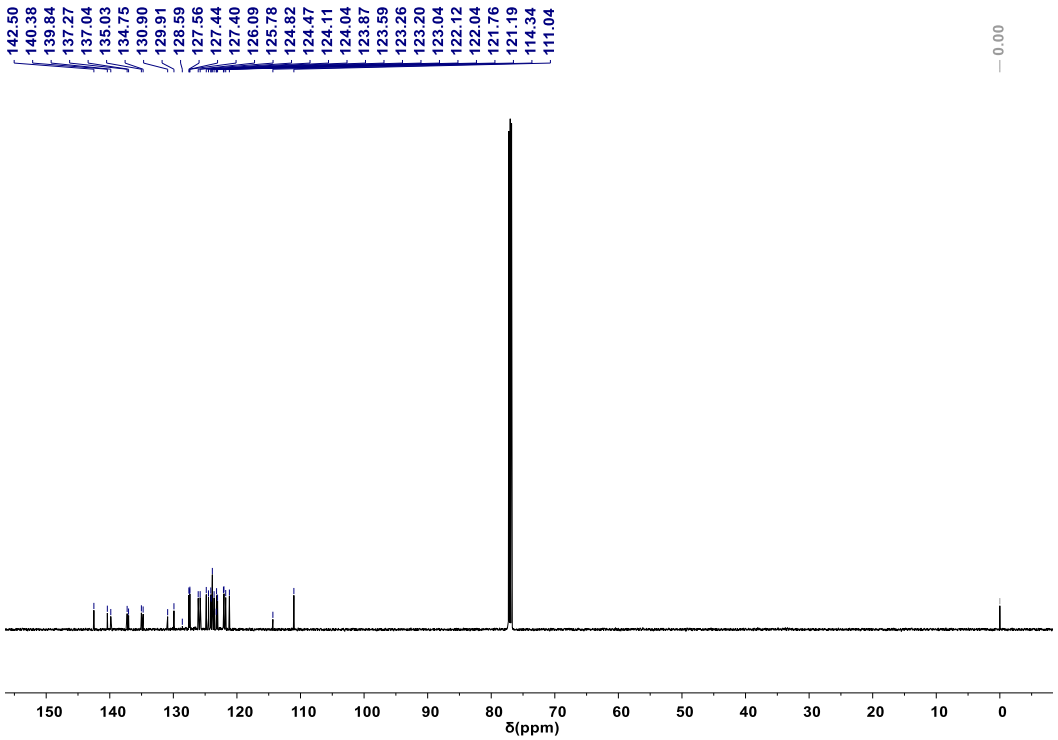

Figure S28. ^{13}C NMR spectrum of the BCzS ($CDCl_3$).

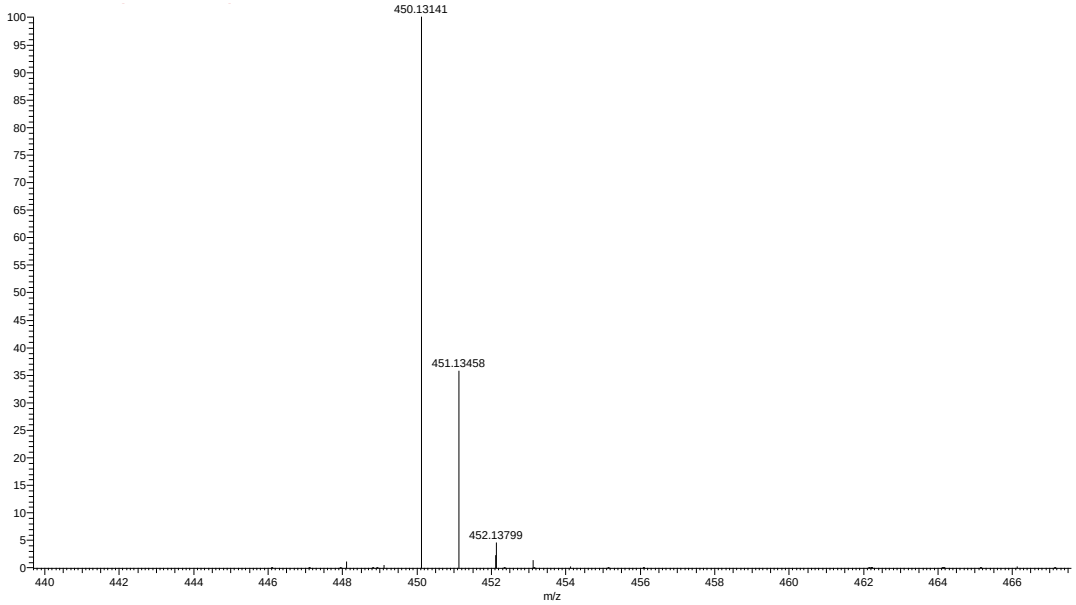

Figure S29. ESI-MS of the BCzS.

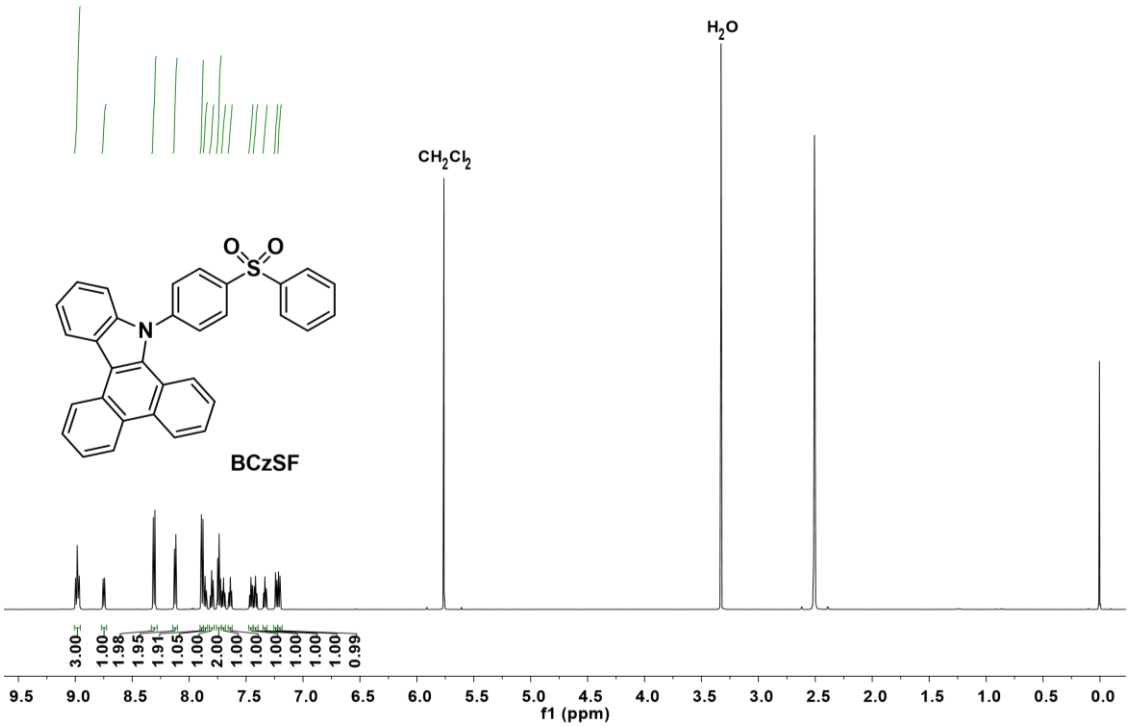

Figure S30. ^{1}H NMR spectrum of the BCzSF (DMSO-d_6).

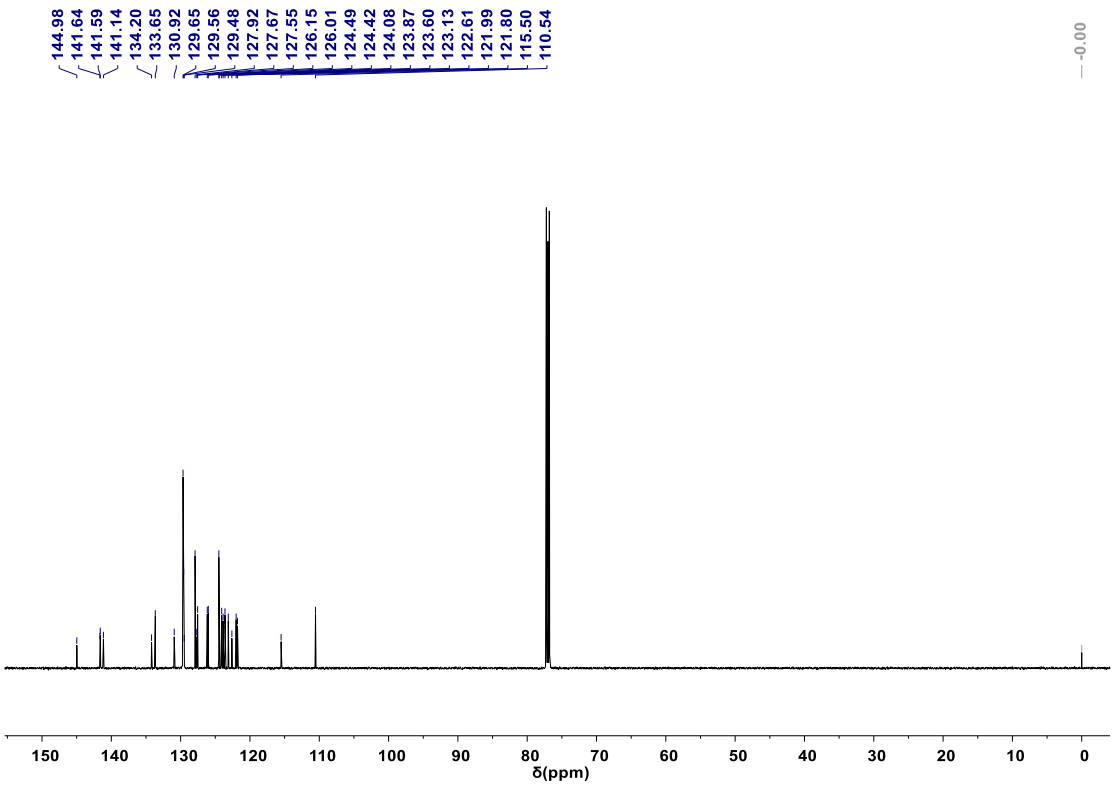

Figure S31. ^{13}C NMR spectrum of the BCzSF ($CDCl_3$).

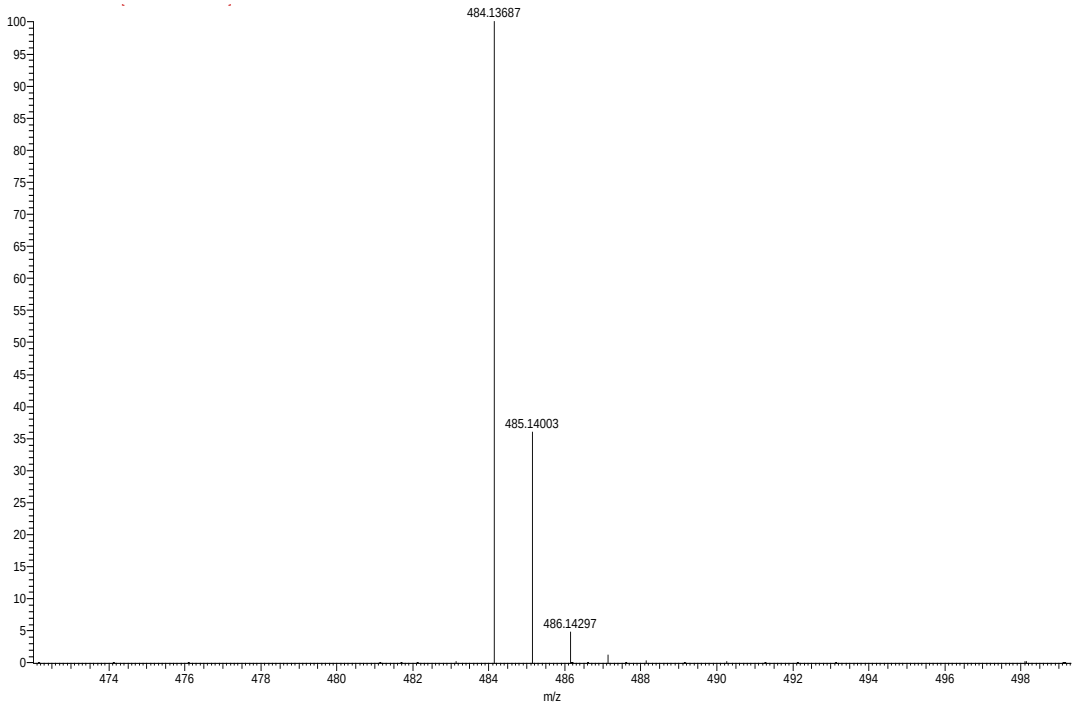

Figure S32. ESI-MS of the BCzSF.

References

1. Y. Ding, X. Wang, M. Tang, H. Qiu, *Adv. Sci.*, 2022, **9**, 2103833.

2. H. Peng, G. Xie, Y. Cao, L. Zhang, X. Yan, X. Zhang, S. Miao, Y. Tao, H. Li, C. Zheng, W. Huang, R. Chen, *Sci. Adv.*, 2022, **8**, eabk2925.

3. W. Dai, G. Li, Y. Zhang, Y. Ren, Y. Lei, J. Shi, B. Tong, Z. Cai, Y. Dong. *Adv. Funct. Mater.*, 2023, **33**, 2210102.

4. M. J. Frisch, G. W. Trucks, H. B. Schlegel, G. E. Scuseria, M. A. Robb, J. R. Cheeseman, G. Scalmani, V. Barone, G. A. Petersson, H. Nakatsuji, X. Li, M. Caricato, A. V. Marenich, J. Bloino, B. G. Janesko, R. Gomperts, B. Mennucci, H. P. Hratchian, J. V. Ortiz, A. F. Izmaylov, J. L. Sonnenberg, Williams, F. Ding, F. Lipparini, F. Egidi, J. Goings, B. Peng, A. Petrone, T. Henderson, D. Ranasinghe, V. G. Zakrzewski, J. Gao, N. Rega, G. Zheng, W. Liang, M. Hada, M. Ehara, K. Toyota, R. Fukuda, J. Hasegawa, M. Ishida, T. Nakajima, Y. Honda, O. Kitao, H. Nakai, T. Vreven, K. Throssell, J. A. Montgomery Jr., J. E. Peralta,

F. Ogliaro, M. J. Bearpark, J. J. Heyd, E. N. Brothers, K. N. Kudin, V. N. Staroverov, T. A. Keith, R. Kobayashi, J. Normand, K. Raghavachari, A. P. Rendell, J. C. Burant, S. S. Iyengar, J. Tomasi, M. Cossi, J. M. Millam, M. Klene, C. Adamo, R. Cammi, J. W. Ochterski, R. L. Martin, K. Morokuma, O. Farkas, J. B. Foresman and D. J. Fox, D. J. *Gaussian 16 Rev. C.01*, Wallingford, CT, 2016.

5. X. Gao, S. Bai, D. Fazzi, T. Niehaus, M. Barbatti and W. Thiel, *J. Chem. Theory Comput.*, 2017, **13**, 515-524.
6. T. Lu and F. Chen, *J. Comput. Chem.*, 2012, **33**, 580-592.
7. W. Humphrey, A. Dalke and K. Schulten, *J. Mol. Graph. Model.*, 1996, **14**, 33-38.
8. Z. Yang, Z. Mao, X. Zhang, D. Ou, Y. Mu, Y. Zhang, C. Zhao, S. Liu, Z. Chi, J. Xu, Y. C. Wu, P. Y. Lu, A. Lien and M. R. Bryce, *Angew. Chem. Int. Ed.*, 2016, **55**, 2181-2185.